Electrochimica Acta 399 (2021) 139440

Contents lists available at ScienceDirect

Electrochimica Acta

journal homepage: www.elsevier.com/locate/electacta

Fabrication of unique porous alumina films with extremely high porosity and an ultra-flat barrier layer by anodizing aluminum in sodium metaborate

Mana Iwai, Tatsuya Kikuchi*

Faculty of Engineering, Hokkaido University, N13-W8, Kita-ku, Sapporo 060-8628, Hokkaido, Japan

ARTICLE INFO

Article history:
Received 1 September 2021
Revised 30 September 2021
Accepted 17 October 2021
Available online 18 October 2021

Keywords:
Anodizing aluminum
Porous oxide film
Sodium metaborate
Keller-Hunter-Robinson Model
High porosity

ABSTRACT

Unique porous anodic aluminum oxide (PAAO) films with a completely flat barrier layer and an extremely porous loofah-like structure were fabricated by anodizing aluminum in an alkaline sodium metaborate solution. High-purity aluminum plates were anodized in a 0.3 M sodium metaborate solution at various applied voltages in the range of 0.1–200 V. A typical PAAO film with a spherical cap barrier layer was formed at voltages lower than 50 V, whereas a PAAO film with a flat barrier layer was formed at voltages higher than 100 V; this film formation was not based on the Keller-Hunter-Robinson model with the spherical barrier layer. The growth interface of the flat barrier layer exhibited an ultra-flat morphology with a minimum roughness value of 0.4 nm, which is much smaller than that of an electropolished aluminum surface. Such barrier layer morphology is expected to be formed by field-assisted dissolution without oxide flow. Although the current density slightly decreased with the applied voltage, a relatively higher current density of 6.8 Am^{-2} was still measured at the lowest voltage of 0.1 V. The alumina walls and the bottom barrier layer gradually thinned as the applied voltage decreased, and a loofah-like PAAO film with an ultra-high porosity of 0.93 was successfully fabricated at 0.1 V. The anodic oxide consisted of amorphous, anion-free aluminum oxide.

1. Introduction

High-aspect-ratio honeycomb alumina structures, known as porous anodic aluminum oxide (PAAO) films, can be fabricated by anodizing aluminum in several suitable acidic electrolyte solutions [1–4]. The morphological characteristics of the PAAO film, such as the interpore distance, pore size, and thickness, are controlled by several operating parameters, such as the applied voltage, temperature, and anodizing time [5–8]. Moreover, advanced anodizing techniques have recently been developed for the fabrication of more complicated nanoporous structures. For example, hard anodizing enables the expansion of the interpore distance due to the higher voltages applied using strong cooling equipment to remove efficiently the Joule heat from the aluminum substrate [9–11]. Pulse anodizing combining hard anodizing with typical anodizing enables the formation of vertically hierarchical pore structures [12–14]. Binary, ternary, and quaternary ordered pore arrays with different morphologies can be fabricated by nanoimprinting before anodizing [15]. Alternating current anodizing leads to laminated porous structures with a beautiful structural color generation [16–18]. Although these novel anodizing methods allow the development of various applications consisting of complicated nanostructures, their structural controllability is inevitably limited because the fabrication process is still based on the typical anodizing method in acidic solutions.

Alkaline electrolyte solutions have not been widely used for anodizing aluminum because of their higher pH values and the corresponding higher solubility of anodic oxides. On the other hand, anodizing aluminum in alkaline solutions has attracted significant attention for the formation of novel anodic oxides. For example, a multilayered alumina film consisting of a plasma electrolytic oxidation layer and a PAAO layer can be fabricated by anodizing in ammonium carbonate [19]. A highly ordered PAAO film with numerous 10 nm scale bumpy alumina walls grows via anodizing in a sodium tetraborate solution [20–22]. This anodizing allows the formation of a porous layer possessing a wide range of interpore distances without the event of oxide burning. Therefore, further research on aluminum anodizing using various alkaline solutions opens the possibility of novel PAAO fabrication.

* Corresponding author.
E-mail address: kiku@eng.hokudai.ac.jp (T. Kikuchi).

https://doi.org/10.1016/j.electacta.2021.139440

Here, we report the fabrication of a new PAAO film, which is different from the typical nanostructure formed in acidic solutions, via anodizing in alkaline sodium metaborate ($NaBO_2$). Sodium metaborate is considered to exhibit the following dissociation reactions in water [23], and the pH of a 0.3 M sodium metaborate solution at 278 K is 11.9, which is a relatively high pH value:

$$NaBO_2 = Na^+ + BO_2^- \quad (1)$$

$$BO_2^- + H_2O = HBO_2 + OH^- \quad (2)$$

$$HBO_2 = BO_2^- + H^+ \quad (3)$$

We found that unique PAAO films with a completely flat barrier layer and an extremely porous loofah-like structure could be fabricated by anodizing in sodium metaborate. Here we describe the details of the PAAO film growth behavior via electrochemical measurements and structural characterization by high-magnification electron microscopy.

2. Experimental

Commercially available 5 N aluminum plates (Nippon Light Metal, 500 μm thick) were cut into rectangular pieces measuring 2 cm in height and 1 cm in width with an electroconductive part. These specimens were immersed in ethanol and ultrasonically washed for 10 min. The bottom electroconductive part was covered with silicone resin after ultrasonication. The specimens were then electropolished in a mixed solution of 22 vol% perchloric acid (70% solution) and 78 vol% acetic acid at 280 K and a constant cell voltage of 28 V for 2 min.

Anodizing was performed using a typical two-electrode system. An electrochemical glass cell was filled with a 0.3 M sodium metaborate electrolyte solution (Kanto chemical, volume: 150 mL), and the aluminum anode and a high-purity platinum cathode (Furuya metal, 3N5, 100 μm thick) were immersed in parallel into the solution (distance: 22 mm). The temperature of the sodium metaborate solution was adjusted to 278–318 K using a constant-temperature water circulator (AS ONE, UCT-1000A). For potentiostatic anodizing of aluminum, the applied voltage was linearly increased to 0.1–200 V in the initial stage of 2.5 min and then was maintained at each setting value for up to 60 min using a direct-current stabilized power supply (Kikusui, PWR400M). The sodium metaborate solution was slowly stirred with a magnetic stirrer bar and a mixer (Thermo Scientific, iMicroStirrer) during anodizing, and the anodizing current was recorded using a digital multimeter (Iwatsu, VOAC7602). Similar potentiostatic anodizing of aluminum in a 0.3 M sulfuric acid solution was carried out to compare the anodizing behaviors.

The anodic oxide films formed under various anodizing conditions were examined by field-emission scanning electron microscopy (FE-SEM, JEOL, JSM6500F) at an accelerating voltage of 10 kV after thin platinum coating. The electroconductive platinum layer (thickness: approximately 10 nm) was coated on the specimen using a magnetron sputter coater (Vacuum device, MSP-1S). The anodic oxide films were chemically dissolved in a mixed solution of 0.2 M chromic acid and 0.51 M phosphoric acid at 353 K, and the exposed aluminum substrate corresponding to the alumina/aluminum interface was examined by atomic force microscopy (AFM, SII, Nanocute). The anodized specimens were embedded in a resin, and ultra-thin sections of the anodic oxide adjusting 25–50 nm in thickness were obtained with trimming glass and diamond knives using an ultramicrotome (RMC, Powertome XL). These ultra-thin sections were examined by Cs-corrected scanning transmission electron microscopy (STEM, FEI, Titan G2 60–300) at an accelerating voltage of 300 kV. Image analysis was performed using image analysis software (Media Cybernetics, Image-Pro 10). The elemental depth-profiling analysis of the anodic oxide was performed using radiofrequency glow discharge optical emission spectroscopy (rf-GDOES, HORIBA, JY-5000RF).

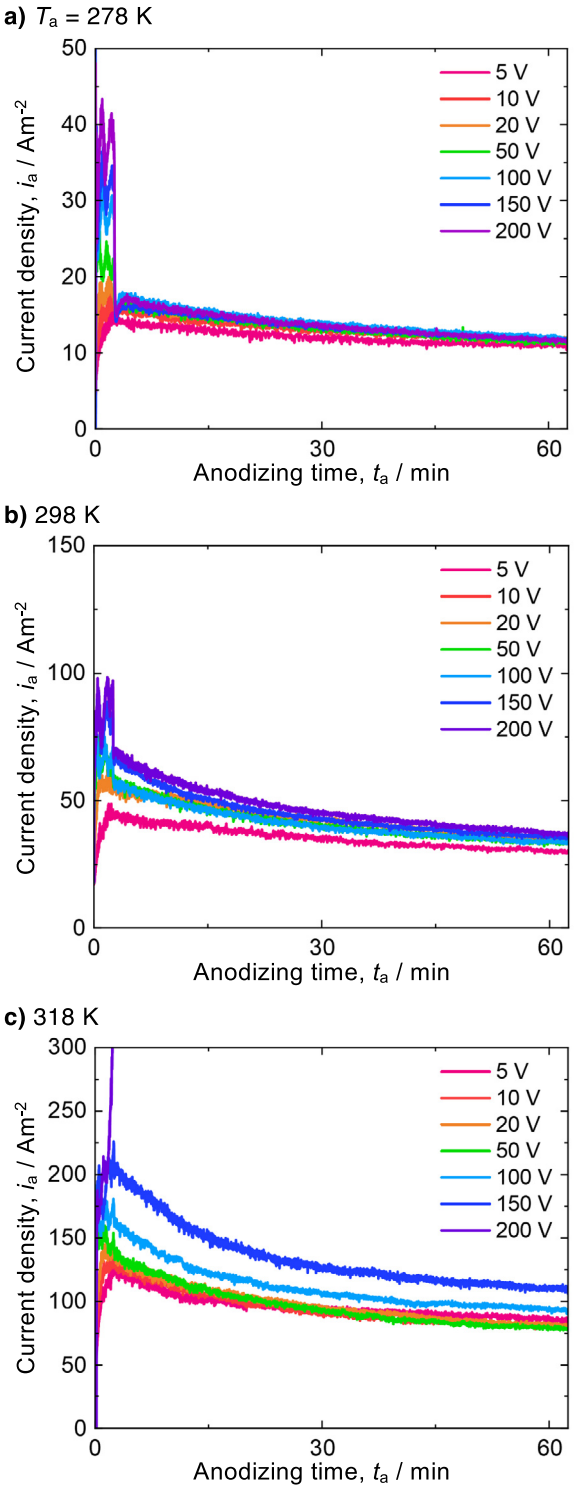

Fig. 1. Current density–time curves measured during potentiostatic anodizing of the electropolished aluminum plates in a 0.3 M sodium metaborate solution at a) 278, b) 298, and c) 318 K for 62.5 min. The current density linearly increased to each target voltage with anodizing time during the initial anodizing period for 2.5 min.

The porosity of the PAAO film is typically measured via SEM image analysis. On the other hand, ultra-thin alumina walls mea-

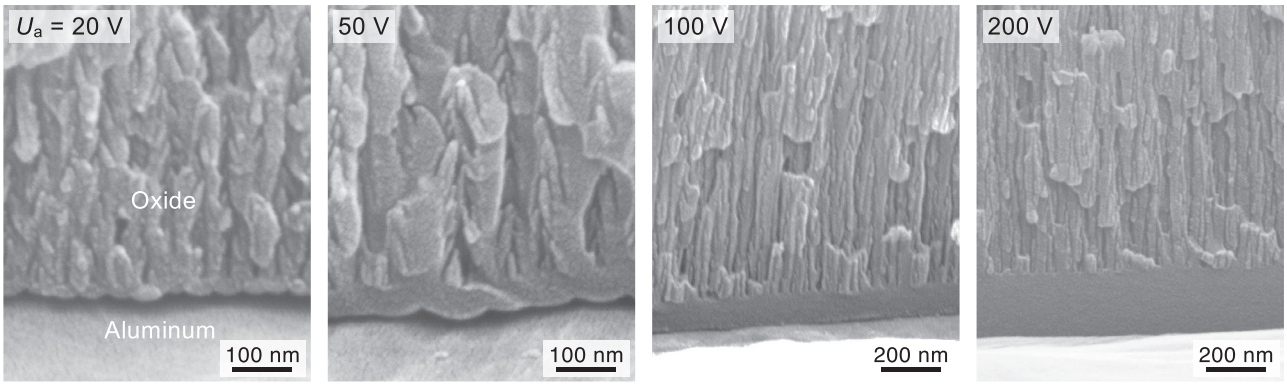

Fig. 2. SEM images of the PAAO films possessing different barrier layer morphologies formed by anodizing in a 0.3 M sodium metaborate solution at 278 K and 20–200 V.

suring less than 5 nm were formed at lower voltages in the present investigation, and such a narrow structure is difficult to evaluate accurately by conventional electron microscopy. Therefore, the porosity of the anodized specimens was measured using the pore-filling method as follows. The aluminum specimens were potentiostatically anodized in a 0.3 M sodium metaborate solution and a 0.3 M sulfuric acid solution at 278 K under various applied voltages. These specimens were immersed in a mixed solution of 0.5 M boric acid and 0.05 M sodium tetraborate at 293 K, and were galvanostatically re-anodized at a constant current density of 5 Am^{-2}. The porosity of the porous layer can be calculated by comparing the two slopes of the voltage–time curves during a) galvanostatic re-anodizing for pore-filling and b) galvanostatic anodizing of the electropolished aluminum specimen. The porosity, α, can be calculated as follows:

$$\alpha = (T_{Al^{3+}} m_2/m_1)/\{1-(1-T_{Al^{3+}})m_2/m_1\} \quad (4)$$

where m_1 is the slope during galvanostatic re-anodizing, m_2 is the slope obtained by galvanostatic anodizing of the electropolished specimen, and $T_{Al}{}^{3+}$ is the transport number of Al^{3+} (0.4). The method is described in detail elsewhere [24,25].

3. Results and discussion

Electrochemical measurements and subsequent nanostructural characterization of the anodic oxide were carried out to understand the anodizing behavior of aluminum in sodium metaborate. Fig. 1a shows the changes in the current density (i_a) with time (t_a) during potentiostatic anodizing at various voltages of U_a = 5–200 V in a 0.3 M sodium metaborate solution at T_a = 278 K (pH = 11.9). At a lower voltage of 5 V, the current density increases to 16 Am^{-2} immediately after the initial linear voltage increased for 2.5 min. The current density then gradually decreases with a slight oscillation, measuring approximately 1–2 Am^{-2}, and reaches a nearly steady-state value of 11 Am^{-2} for 62.5 min. The current density increased only slightly with the applied voltage, although there were no significant changes in the shape of the current density–time curves obtained at each voltage. Therefore, the anodic oxide growth rate is expected to be almost independent of the applied voltage at this low temperature. As the temperature of the sodium metaborate solution was increased to 298 K and 318 K (Figs. 1b and 1c), the current densities increased with temperature and were approximately three to nine times larger than that at 278 K. Conversely, anodizing at a higher temperature of 318 K and a higher voltage of 200 V led to oxide burning with a significant increase in the current in the early stage. Anodizing at higher temperatures caused the chemical dissolution of the top anodic oxide due to the higher pH of the alkaline sodium metaborate solution. At the same electrolyte temperature, there was still a small difference in the current density, even though the applied voltage increased by a factor of ten or more. However, we found that the morphologies of the anodic oxides grown at lower and higher voltages were significantly different.

The specimens anodized in sodium metaborate solution at 278 K and 20–200 V for 62.5 min were bent to exposure the cross-section of the anodic oxide, and these oxide films were examined by SEM (Fig. 2). A PAAO film consisting of an outer thick porous layer and an inner thin barrier layer was observed at lower applied voltages of 20 V and 50 V. Although the pores had a very small and twisted shape, without a clear straight morphology, these anodic oxides were very similar to the typical disordered PAAO films obtained by anodizing in acidic electrolyte solutions [26]. As the applied voltage increased to 100 V, the nanopores formed in the porous layer became quite linear. Characteristically, the morphology of the inner barrier layer changed from a spherical cap structure to a flat, smooth film similar to the barrier oxide film formed by anodizing in neutral solutions such as borate and adipate [27,28]. The thickness of the flat barrier layer doubled as the applied voltage increased to 200 V, whereas there was no significant change in the outer porous layer. In the general anodizing process for the growth of PAAO films, the size of the inner spherical cap barrier layer increases with the applied voltage while maintaining their morphology [1]. Therefore, we expected unconventional growth behavior to occur during anodizing in a sodium metaborate solution. To investigate the nanomorphology of these anodic oxides in detail, the specimens were examined using high-magnification STEM observations.

Fig. 3 shows high-angle annular dark-field (HAADF) STEM images of the inner and middle layers of the PAAO film formed at a low voltage of 20 V. The top image shows a spherical cap barrier oxide array at the bottom of the pores, and this morphology is very similar to that of the typical PAAO film. It has been previously reported that the thickness of the bottom barrier layer (t_b) is proportional to the applied voltage during anodizing [1,29]:

$$t_b = kU_a \quad (5)$$

where k is a proportional constant (anodizing ratio). The anodizing ratio obtained in various acidic electrolyte solutions has been reported to be approximately 1.0. However, the thickness of the barrier layer and the corresponding anodizing ratio formed in the sodium metaborate solution were calculated to be 34 nm and 1.7, respectively, and these values are much larger than those of typical PAAO films. Similar thickening of the barrier layer was also measured in the PAAO film prepared using an alkaline sodium tetraborate solution [22]. In addition, the wall surface of the pores had a non-uniform shape with many nanometer-/tens of nanometer-scale bumps. Such a bumpy pore morphology is similar to that of the PAAO film formed in chromic acid and sodium tetraborate

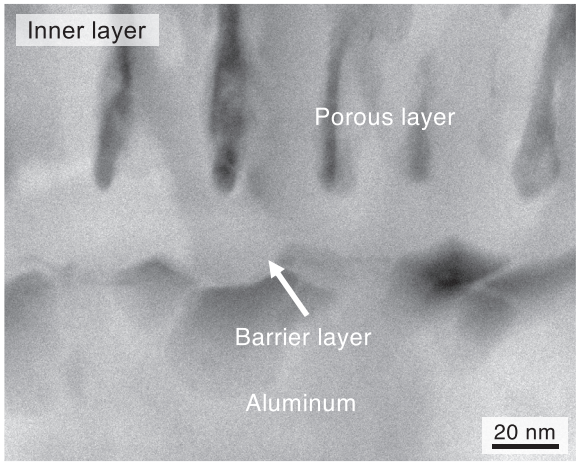

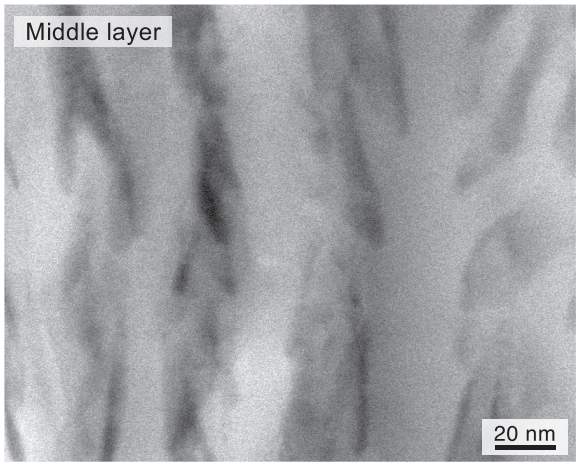

Fig. 3. HAADF-STEM images of the inner and middle layers of the PAAO film formed by anodizing in a 0.3 M sodium metaborate solution at 278 K and 20 V.

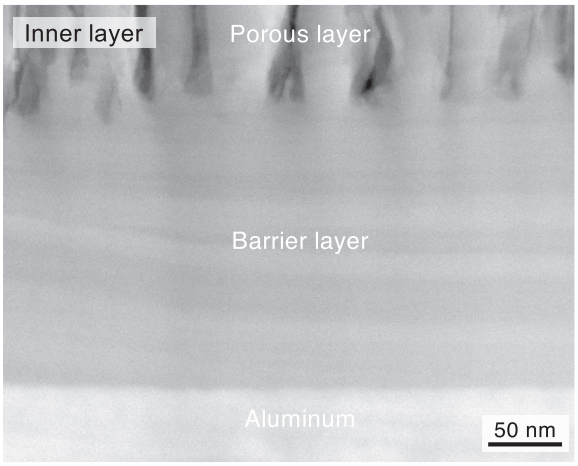

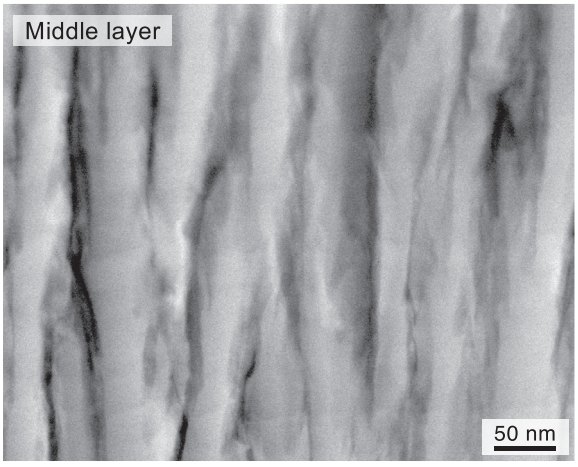

Fig. 4. HAADF-STEM images of the inner and middle layers of the PAAO film formed by anodizing in a 0.3 M sodium metaborate solution at 278 K and 200 V.

[22,30–32]. Based on the high-magnification STEM observations, the nanostructure of the PAAO film obtained in sodium metaborate at lower voltages is close to the shape of a typical PAAO film, although the anodizing ratio and pore wall morphology are different.

Fig. 4 shows high-magnification HAADF-STEM images of the PAAO film obtained at 200 V. Unlike the PAAO film obtained at lower voltages, there is no spherical cap barrier layer at the bottom of the porous layer. A characteristic uniform barrier oxide film with a thickness of 254 nm can be observed, and the interfaces at the porous layer/barrier layer and the barrier layer/aluminum substrate possess a flat feature. The calculated anodizing ratio of this barrier layer was approximately 1.3, which was also larger than that of typical PAAO films formed in acidic solutions. Although the pores grew more linearly than those at 20 V, the entire pore walls also had a bumpy surface with a branching structure.

Fig. 5a shows SEM images of the barrier layer/aluminum substrate interface formed at 20–200 V after the chemical removal process of anodic oxides. Numerous disordered dimples with an average diameter of 52 nm, which corresponds to the bottom morphology of the spherical cap barrier layer, were distributed on the aluminum surface at 20 V. This morphology is consistent with the typical nanostructure of PAAO films [33,34]. However, the boundaries of these dimples became slightly unclear as the applied voltage increased to 50 V. Moreover, there was no clear unevenness at applied voltages greater than 100 V. Fig. 5b shows two- and three-dimensional height images of the aluminum surface measured by AFM, and a vertical color bar represents the height in the range of 0–30 nm. Clear bumpy structures measuring 2.7–2.8 nm in surface roughness (Ra) were formed at lower voltages of 20 V and 50 V. These bumpy structures almost disappeared at higher voltages of 100 V and 200 V, and extremely smooth aluminum surfaces with a surface roughnesses of 0.6 nm and 0.4 nm, respectively, were obtained. These values were significantly smaller than those obtained on the original electropolished aluminum surface with a nanoscale pattern (Ra = 1.0 nm), and these specimens may be useful as ultra-smooth aluminum surfaces.

Based on the experimental results described above, the nanomorphology of the bottom barrier layer formed by anodizing in sodium metaborate solution is significantly different at lower and higher voltages; the spherical cap barrier layer was formed at lower voltages, and a flat barrier layer was obtained at higher voltages (Fig. 6). In contrast, a similar porous layer with bumpy alumina walls was formed on the barrier layer at each applied voltage. The nanoscale honeycomb structure of the PAAO film formed by anodizing in typical acidic solutions was first revealed using an electron microscope by Keller, Hunter, and Robinson (KHR) in 1953 [35]. According to the KHR model, PAAO films are composed of an array of numerous hexagonal unit cells consisting of a nanoscale pore at its center, an alumina wall surrounding the pore, and a thin barrier layer with a spherical cap structure at its base. During anodizing, the anions and cations are isotropically conducted in the hemispherical cap barrier alumina layer under high electric field conditions [29]. The KHR model agrees well with the anodic oxide formed in sodium metaborate at less than 50 V (Fig. 3). However, the morphology of the bottom barrier layer formed at more than

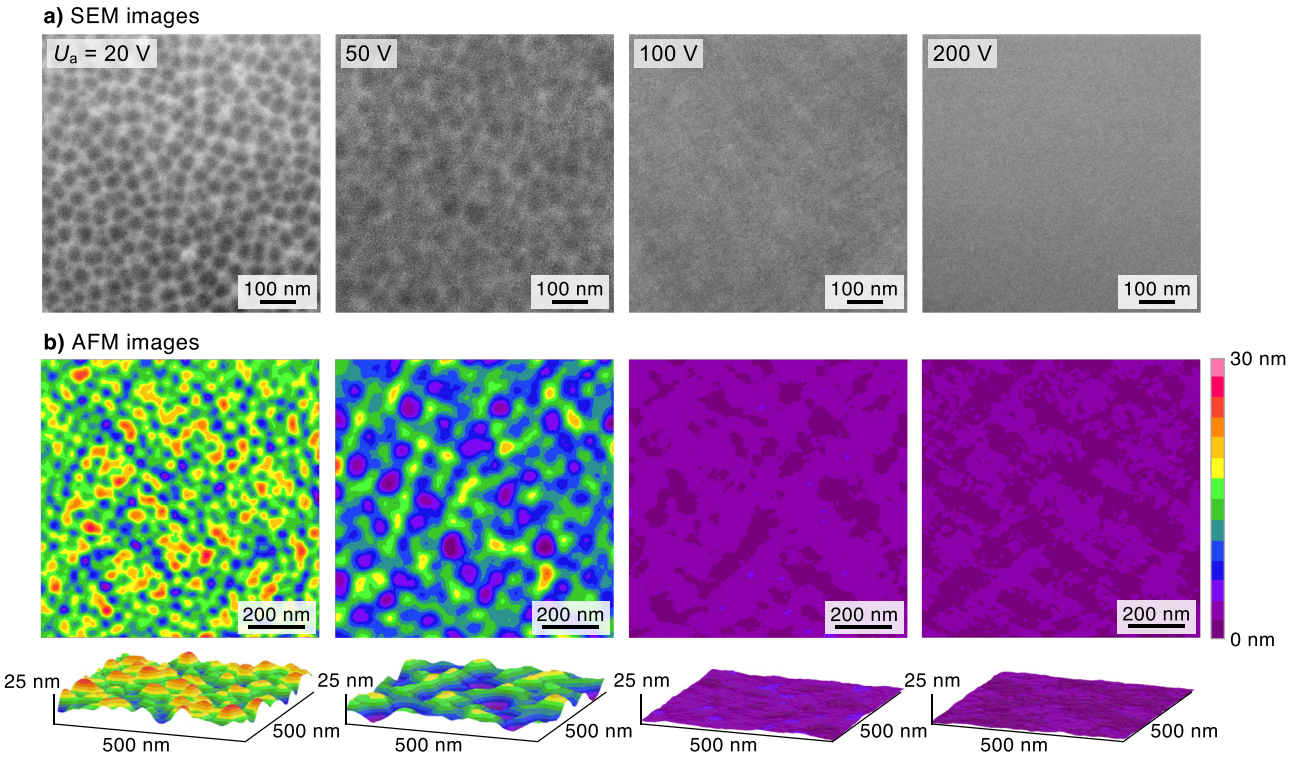

Fig. 5. a) SEM and b) AFM images of the aluminum surface exposed by the chemical dissolution of the PAAO film after anodizing in a 0.3 M sodium metaborate solution at 278 K and 20–200 V for 62.5 min.

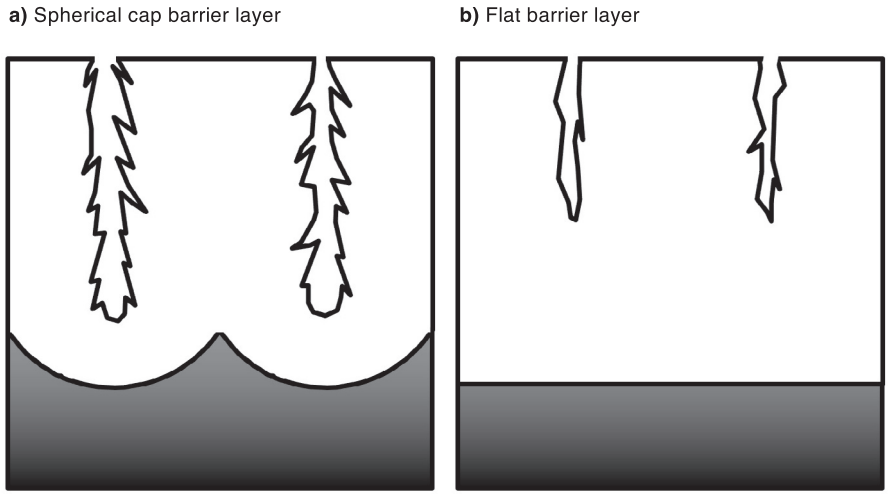

Fig. 6. Schematic models of the two types of PAAO film with a) a spherical cap barrier layer corresponding to the KHR model and b) a flat barrier layer that differs from the traditional KHR model.

100 V is not based on the traditional porous oxide shape reported by KHR (Fig. 4).

Similar PAAO films with a flat barrier layer can be formed by galvanostatic re-anodizing in a neutral solution after first anodizing in an acidic solution to form a typical PAAO film [36]. In this re-anodizing process, the morphology of the spherical cap barrier layer gradually changes to a flat alumina film as the applied voltage increases. During this re-anodizing process in a neutral solution, the barrier layer can be thickened up to several hundred nanometers without film breakdown, whereas the porous layer is unchanged; thus, the total thickness of the PAAO film increases slightly by re-anodizing. Conversely, we found that the porous layer formed in sodium metaborate at higher voltages thickened with anodizing time. Fig. 7 shows SEM images of the cross-section of the PAAO film formed at 200 V for 12.5, 32.5, and 62.5 min. A PAAO film consisting of a 310 nm-thick outer porous layer and a 240 nm-thick inner flat barrier layer was observed for 12.5 min. Although the thickness of the barrier layers was unchanged at 240 nm as the anodizing time increased, the thickness of the porous layer gradually increased to 820 nm for 32.5 min and 1.6 μm for 62.5 min with the anodizing time. Thus, steady-state growth of the outer porous layer possessing a flat barrier oxide with a constant thickness occurs during anodizing at higher voltages.

The PAAO film with the flat barrier layer is formed at higher voltages due to the different formation mechanism of the bottom alumina layer. The field-assisted dissolution model and flow model are well accepted as the formation mechanisms of PAAO films [29].

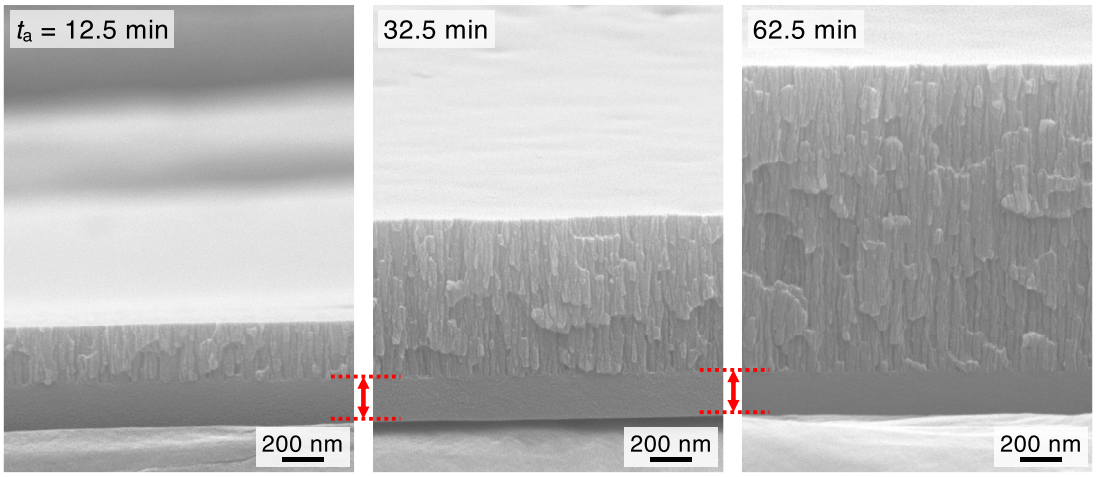

Fig. 7. Time variation of the PAAO film with the flat barrier layer during anodizing in a 0.3 M sodium metaborate solution at 278 K and 200 V for 12.5, 32.5, and 62.5 min.

Recently, Thompson and Hebert suggested a flow model of anodic oxides at high electric fields during anodizing in acidic electrolyte solutions [37–42]. This oxide flow occurs by non-uniform compressive stress at the interface between the electrolyte solution and the anodic oxide owing to anion adsorption; thus, the PAAO film consists of nanoscale pores and spherical cap barrier oxides at the pore bottom. This morphology corresponds to the shape of the PAAO film formed in sodium metaborate at low voltages. In contrast, Thompson reported a re-anodizing method to separate the flow model and field-assisted growth instabilities [43]. In this process, an aluminum plate is anodized in a neutral solution to form a flat barrier oxide film, and then the specimen is re-anodized in an acidic solution to form a PAAO film. They found that disordered pores were formed on the flat pre-formed barrier oxide film using the field-assisted dissolution model. Therefore, the characteristic PAAO films with a flat barrier layer obtained in sodium metaborate at higher voltages may be formed by the field-assisted dissolution model without oxide flow. The morphology may be gradually changed to the flat oxide from the spherical cap barrier layer at the middle voltage range of 50–100 V.

As shown in Fig. 1a, the current densities remain approximately unchanged with increasing applied voltage during anodizing in a 0.3 M sodium metaborate solution at 278 K. Conversely, the growth behavior of the PAAO film when the voltage decreased was investigated in detail. Fig. 8 shows the i_a– t_a curves during potentiostatic anodizing at 0.1–5 V in a) a 0.3 M sulfuric acid solution and b) a 0.3 M sodium metaborate solution at 278 K. Here, sulfuric acid, typically used for anodizing at low applied voltages, was employed for comparison. At an applied voltage of 5 V in sulfuric acid (Fig. 8a), the current density in the steady-state region is approximately 2.0 Am^{-2}. The current density gradually decreases with the applied voltage, and an extremely low current density of 0.4 Am^{-2} is observed at 0.1 V. Thus, the growth rate of the anodic oxide is expected to be extremely slow during anodizing in a sulfuric acid solution at lower voltages. In contrast, the current density only slightly decreases as the applied voltage decreases in a sodium metaborate solution, and a relatively large current density of 6.8 Am^{-2} is retained at 0.1 V. Comparing the same applied voltages, the anodic oxide formed in sodium metaborate grew 5–17 times faster than that in sulfuric acid, and this rapid growth rate obtained in sodium metaborate is an advantage for the fabrication of small-scale PAAO films.

Fig. 9 shows high-magnification HAADF-STEM images of the PAAO films formed in sodium metaborate at low applied voltages of a) 3, b) 1, and c) 0.1 V. A remarkably branched PAAO film with

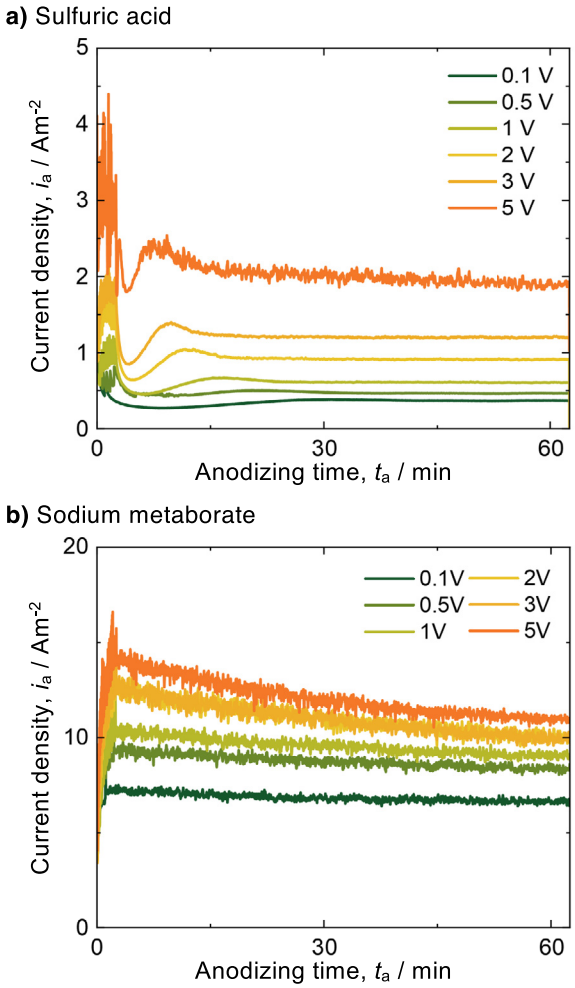

Fig. 8. Current density–time curves measured during potentiostatic anodizing of the electropolished aluminum plates in a) a 0.3 M sulfuric acid solution at 278 K and b) a 0.3 M sodium metaborate solution at 278 K for 62.5 min.

thin alumina walls can be observed at 3 V (Fig. 9a). The alumina walls become notably thinner as the applied voltage decreases to 1 V (Fig. 9b), and this unique nanomorphology is similar to the sponge-like internal structure of loofahs. As the voltage further decreases to 0.1 V (Fig. 9c), a highly porous oxide film with ultra-

Table 1
Summary of the barrier layer morphology and the porosity of the PAAO film obtained by anodizing in a 0.3 M sodium metaborate solution at 278 K.

Applied voltage	0.1	0.5	1	2	3	5	10	20	50	100	150	200
Barrier layer morphology	spherical	spherical	spherical	spherical	spherical	spherical	spherical	spherical	spherical	flat	flat	flat
Porosity	0.926	0.835	0.718	–	–	–		0.190	0.162	0.156	0.157	0.181

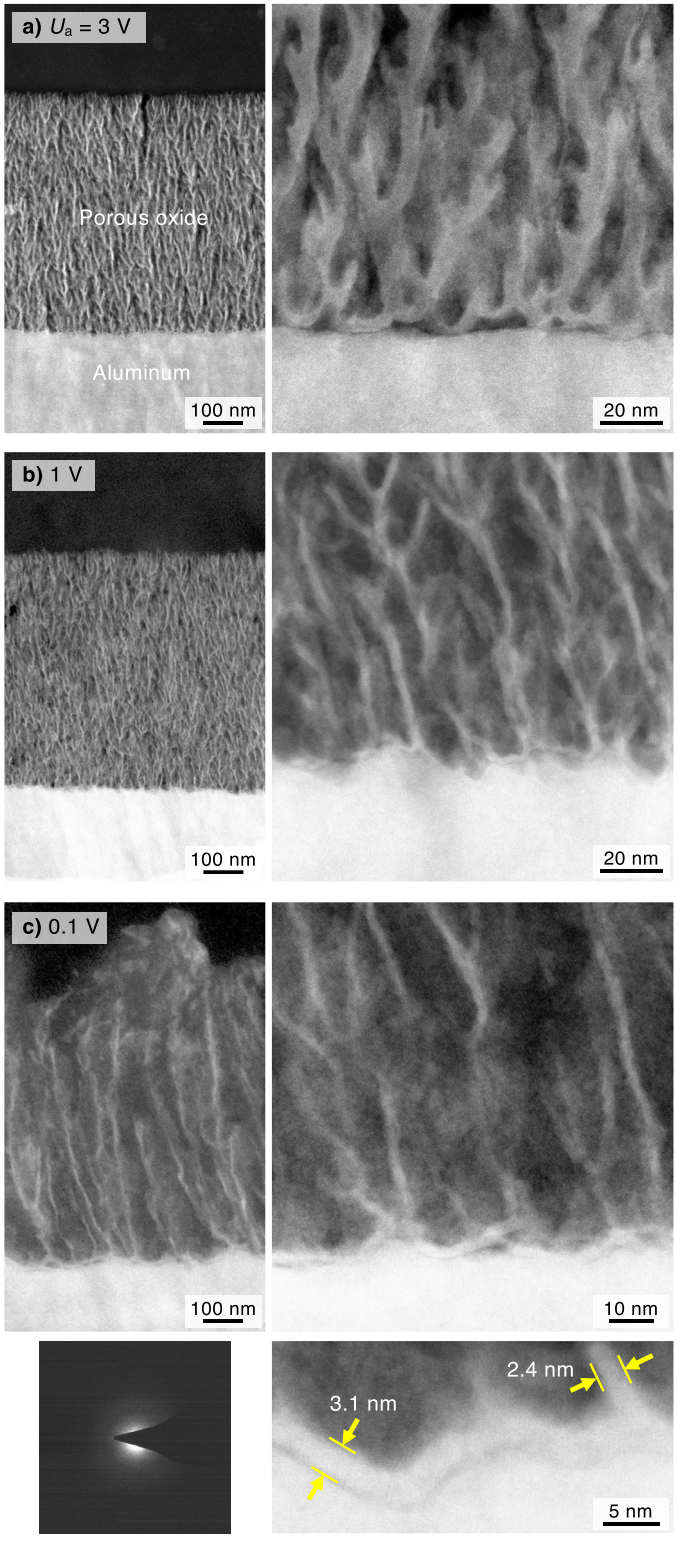

Fig. 9. Low- and high-magnification HAADF-STEM images of the PAAO film formed by anodizing in a 0.3 M sodium metaborate solution at 278 K and a) 3, b) 1, and c) 0.1 V. A corresponding diffraction pattern of the anodic oxide formed at 0.1 V is shown in c).

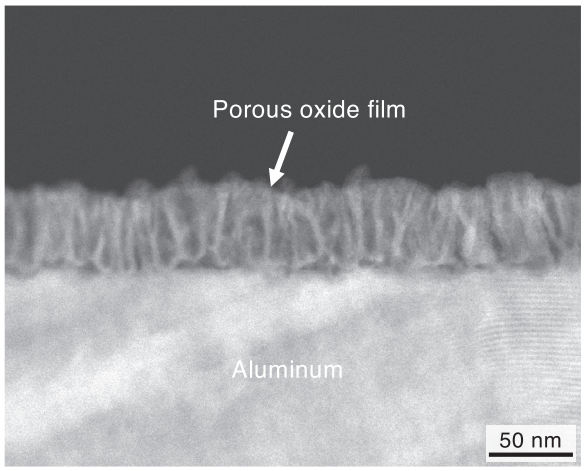

Fig. 10. HAADF-STEM image of the PAAO film formed by anodizing in a 0.3 M sulfuric acid at 278 K and 0.1 V.

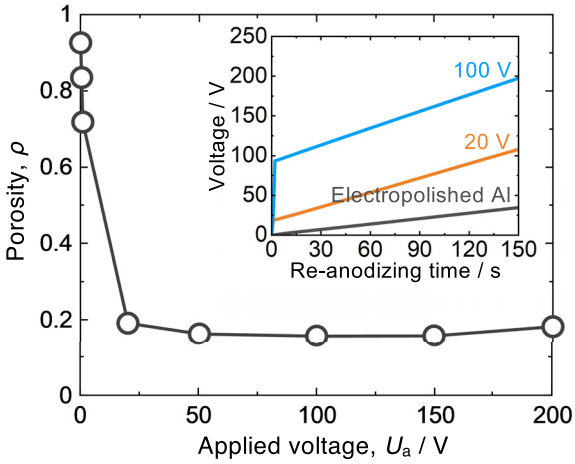

Fig. 11. Change in the porosity of the PAAO film formed in a 0.3 M sodium metaborate solution at 278 K with the applied voltage. The porosity was calculated by the pore-filling method. The insert figure shows the voltage–time curves during galvanostatic re-anodizing for pore-filling and galvanostatic anodizing of the electropolished specimen.

thin alumina walls and barrier layers measuring 2.4 nm and 3.1 nm can be observed on the aluminum surface. In this observation, the top surface of the PAAO film is slightly deformed by the irradiation of the electron beam owing to its low porosity. In comparison with the PAAO film formed by anodizing in sulfuric acid at the same applied voltage of 0.1 V (Fig. 10), it seems that the PAAO film formed in sodium metaborate has a thicker layer and a higher porosity. The electron diffraction pattern of the PAAO films formed in sodium metaborate exhibits an amorphous structure with a halo feature.

To investigate the effect of the applied voltage on the porosity of the PAAO film, the aluminum specimens were anodized in a 0.3 M sodium metaborate solution at 278 K and various voltages in the range of 0.1–200 V, and then the porosities of the fabricated PAAO films were measured by the pore-filling method. Fig. 11 summarizes the changes in the porosity (ρ) according to the

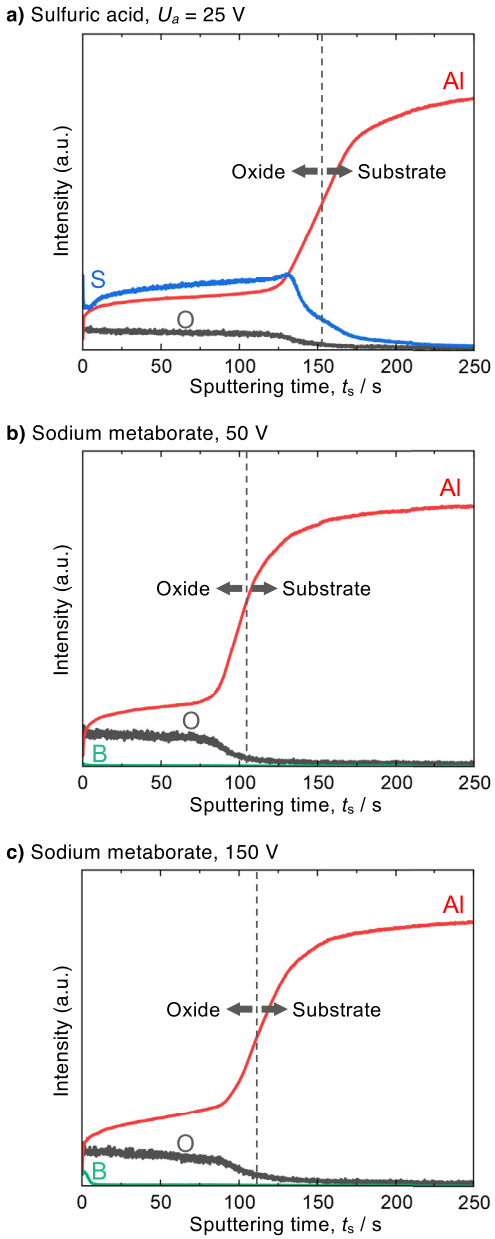

Fig. 12. GDOES depth profiles of aluminum, oxygen, sulfur, and boron in the PAAO films formed in a) a 0.3 M sulfuric acid solution at 283 K and 25 V, b) a 0.3 M sodium metaborate solution at 278 K and 50 V, and c) a 0.3 M sodium metaborate solution at 278 K and 150 V.

applied voltage. The PAAO films exhibit an almost steady porosity of 0.16–0.19 at applied voltages greater than 20 V; thus, the porosity was also independent of the morphology of the bottom barrier oxide film (i.e., the spherical cap barrier layer and the flat barrier layer). Conversely, the porosity significantly increases with decreasing applied voltage, and the PAAO films with high porosities measuring 0.93 and 0.84 were successfully fabricated by anodizing in sodium metaborate solution at 0.1 V and 0.5 V, respectively. It is considered that this value is good agreement with the morphology of the PAAO film shown in Fig. 9c. Because the porosity of the PAAO film formed in sulfuric acid at 0.1 V (Fig. 10) was 0.65, an extremely high porosity could be achieved by anodizing in sodium metaborate. It has been previously reported that PAAO films with high porosities can be fabricated by typical anodizing at high temperatures or subsequent pore widening in an alumina etching solution. However, because higher temperature and excess pore widening lead to the disappearance of the porous structure, the maximum porosity was still limited to approximately 0.32–0.54 [44,45]. Therefore, anodizing in sodium metaborate is useful for the fabrication of PAAO films with significantly higher porosity at a rapid growth rate than conventional anodizing methods. The barrier layer morphology and the porosity of the PAAO film obtained by anodizing in a 0.3 M sodium metaborate solution at 278 K were summarized in Table. 1.

Fig. 12 shows the rf-GDOES depth profiles of the specimens anodized in a) 0.3 M sulfuric acid solution at 293 K and 25 V for 10 min, b) 0.3 M sodium metaborate solution at 278 K and 50 V, and c) 0.3 M sodium metaborate solution at 278 K and 150 V for 62.5 min. Typical PAAO films formed in acidic solutions, such as sulfuric acid, have electrolyte anions incorporated into their alumina structure [46]. Therefore, sulfur originating from the sulfate anions was measured throughout the vertical region of the PAAO film formed in sulfuric acid (Fig. 12a). In contrast, the PAAO films formed in sodium metaborate consisted of anion-free aluminum oxide, although boron was measured slightly near the surface due to the adsorption of the electrolyte anions (Figs. 12b and 12c). The difference in the morphology of the barrier layer did not affect the anion incorporation, and PAAO films consisting of pure aluminum oxide were fabricated by anodizing in sodium metaborate. It has been reported that impurity-free PAAO films can be fabricated by anodizing in a chromic acid solution [32,47]. However, the use of hexavalent chromium should be avoided for global environmental protection. Therefore, PAAO films consisting of impurity-free, pure aluminum oxide, formed by environmentally friendly anodizing in sodium metaborate, may be useful for various basic research and industrial applications.

4. Conclusions

We described the structural characterization of a PAAO film formed by anodizing aluminum in a 0.3 M sodium metaborate solution with a relatively higher pH value of approximately 12, and found that unique PAAO films could be fabricated under various applied voltages. A PAAO film consisting of an outer bumpy, porous layer and an inner hemispherical cap barrier layer, which is similar to the typical PAAO films formed in acidic solutions, was formed at lower voltages below 50 V. In contrast, a PAAO film possessing a flat barrier layer, which is different from the typical KHR model, was obtained at voltages higher than 100 V, and the growth interface exhibited an extremely flat morphology with a roughness of 0.4–0.6 nm, which is lower than that obtained on electropolished aluminum surfaces (1.0 nm). The porosities of the porous layer obtained above 20 V were almost constant (0.16–0.19). However, the porosity increased significantly at lower applied voltages. Moreover, a unique loofah-like PAAO film with an extremely high porosity of 0.93 can be fabricated at 0.1 V. The current density corresponding to the growth rate of the PAAO film at this voltage was 17 times higher than that of typical sulfuric acid. The anodic oxide formed in sodium metaborate consisted of amorphous, anion-free aluminum oxide.

Declaration of Competing Interest

The authors declare no competing interests.

Credit authorship contribution statement

Mana Iwai: Conceptualization, Data curation, Funding acquisition, Investigation, Methodology, Visualization, Writing – original draft. **Tatsuya Kikuchi:** Conceptualization, Funding acquisi-

tion, Methodology, Project administration, Supervision, Visualization, Writing – review & editing.

Acknowledgments

The authors acknowledge financial support from the Light Metal Educational Foundation Japan, the Japan Society for the Promotion of Science KAKENHI (grant number: 19H02470), and the Nanotechnology Platform Japan (grant number: A-21-HK-0001). We also thank Prof. Hiroki Habazaki, Mr. Satoru Kimura, Dr. Takashi Endo, and Mr. Ryo Oota (Hokkaido University) for their technical support in the GDOES measurements and SEM/STEM observations.

References

[1] S.Z. Chu, K. Wada, S. Inoue, M. Isogai, Y. Katsuta, A. Yasumori, Large-scale fabrication of ordered nanoporous alumina films with arbitrary pore intervals by critical-potential anodization, J. Electrochem. Soc. 153 (2006) B384.
[2] T. Kikuchi, D. Nakajima, O. Nishinaga, S. Natsui, R.O. Suzuki, Porous aluminum oxide formed by anodizing in various electrolyte species, Curr. Nanosci. 11 (2015) 560.
[3] A. Ruiz-Clavijo, O. Caballero-Calero, M. Martín-González, Revisiting anodic alumina templates: from fabrication to applications, Nanoscale 13 (2021) 2227.
[4] M. Pashchanka, Conceptual progress for explaining and predicting self-organization on anodized aluminum surfaces, Nanomaterials 11 (2021) 2271.
[5] G.D. Sulka, K.G. Parkoła, Temperature influence on well-ordered nanopore structures grown by anodization of aluminium in sulphuric acid, Electrochim. Acta 52 (2007) 1880.
[6] G.D. Sulka, W.J. Stępniowski, Structural features of self-organized nanopore arrays formed by anodization of aluminum in oxalic acid at relatively high temperatures, Electrochim. Acta 54 (2009) 3683.
[7] M. Iwai, T. Kikuchi, R.O. Suzuki, S. Natsui, Electrochemical and morphological characterization of porous alumina formed by galvanostatic anodizing in etidronic acid, Electrochim. Acta 320 (2019) 134606.
[8] T. Kikuchi, A. Takenaga, S. Natsui, R.O. Suzuki, Advanced hard anodic alumina coatings via etidronic acid anodizing, Surf. Coat. Technol. 326 (2017) 72.
[9] W. Lee, R. Ji, U. Gösele, K. Nielsch, Fast fabrication of long-range ordered porous alumina membranes by hard anodization, Nat. Mater. 5 (2006) 741.
[10] K. Schwirn, W. Lee, R. Hillebrand, M. Steinhart, K. Nielsch, U. Gösele, Self-ordered anodic aluminum oxide formed by H_2SO_4 hard anodization, ACS Nano 2 (2008) 302.
[11] W. Lee, J.C. Kim, U. Gösele, Spontaneous current oscillations during hard anodization of aluminum under potentiostatic conditions, Adv. Funct. Mater. 20 (2010) 21.
[12] W. Lee, K. Schwirn, M. Steinhart, E. Pippel, R. Scholz, U. Gösele, Structural engineering of nanoporous anodic aluminium oxide by pulse anodization of aluminium, Nat. Nanotechnol. 3 (2008) 234.
[13] G.D. Sulka, A. Brzózka, L. Liu, Fabrication of diameter-modulated and ultrathin porous nanowires in anodic aluminum oxide templates, Electrochim. Acta. 56 (2011) 4972.
[14] J. Martín, M. Martín-González, J.F. Fernández, O. Caballero-Calero, Ordered three-dimensional interconnected nanoarchitectures in anodic porous alumina, Nat. Commun. 5 (2014) 5130.
[15] L. Wen, R. Xu, Y. Mi, Y. Lei, Multiple nanostructures based on anodized aluminium oxide templates, Nat. Nanotechnol. 12 (2017) 244.
[16] M. Ishino, H. Hashimoto, H. Asoh, Effect of cathodic current on the structural features of oxide films formed by AC anodization of aluminum, J. Electrochem. Soc. 164 (2017) C939.
[17] H. Segawa, K. Wada, Structural colors of laminated alumina films prepared by ac oxidation in oxalic acid solution, Mater. Chem. Phys. 250 (2020) 123031.
[18] H. Segawa, K. Wada, Shiny laminated alumina films prepared by ac oxidation, Mater. Chem. Phys. 242 (2020) 122534.
[19] T. Kikuchi, T. Taniguchi, R.O. Suzuki, S. Natsui, Fabrication of a plasma electrolytic oxidation/anodic aluminum oxide multi-layer film via one-step anodizing aluminum in ammonium carbonate, Thin Solid Films 697 (2020) 137799.
[20] S.J. Garcia-Vergara, P. Skeldon, G.E. Thompson, H. Habakaki, Pore development in anodic alumina in sulphuric acid and borax electrolytes, Corr. Sci. 49 (2007) 3696.
[21] T. Kikuchi, K. Kunimoto, H. Ikeda, D. Nakajima, R.O. Suzuki, S. Natsui, Fabrication of anodic porous alumina via galvanostatic anodizing in alkaline sodium tetraborate solution and their morphology, J. Electroanal. Chem. 846 (2019) 113152.
[22] M. Iwai, T. Kikuchi, R.O. Suzuki, Self-ordered nanospike porous alumina fabricated under a new regime by an anodizing process in alkaline media, Sci. Rep. 11 (2021) 7240.
[23] T. Yasunaga, N. Tatsumoto, M. Miura, Ultrasonic absorption in sodium metaborate solution, J. Chem. Phys. 43 (1965) 2735.
[24] H. Takahashi, M. Nagayama, The determination of the porosity of anodic oxide films on aluminium by the pore-filling method, Corr. Sci. 18 (1978) 911.
[25] M. Matsumoto, H. Hashimoto, H. Asoh, Formation efficiency of anodic porous alumina in sulfuric acid containing alcohol: comparison of the effects of monohydric and polyhydric alcohols as additives, J. Electrochem. Soc. 167 (2020) 041504.
[26] M. Iwai, T. Kikuchi, R.O. Suzuki, Initial Structural Changes of porous alumina film via high-resolution microscopy observations, ECS J. Solid State Sci. Technol. 9 (2020) 044004.
[27] H. Takahashi, M. Nagayama, Electrochemical behaviour and structure of anodic oxide films formed on aluminium in a neutral borate solution, Electrochim. Acta 23 (1978) 279.
[28] C. M. J.K. Chang, C.M Lin, C.H. Liao, W.T Chen, Tsai, Effect of heat-treatment on characteristics of anodized aluminum oxide formed in ammonium adipate solution, J. Electrochem. Soc. 151 (2004) B188.
[29] W. Lee, S.J. Park, Porous anodic aluminum oxide: anodization and templated synthesis of functional nanostructures, Chem. Rev. 114 (2014) 7487.
[30] S.J. Garcia-Vergara, P. Skeldon, G.E. Thompson, H. Habazaki, A tracer investigation of chromic acid anodizing of aluminium, Surf. Interdface Anal. 39 (2007) 860.
[31] D. Elabar, A. Němcová, T. Hashimoto, P. Skeldon, G.E. Thompson, Effect of sulphate impurity in chromic acid anodizing of aluminium, Corr. Sci. 100 (2015) 377.
[32] T. Kikuchi, M. Yamashita, M. Iwai, R.O. Suzuki, Self-ordering of porous anodic alumina fabricated by anodizing in chromic acid at high temperature, J. Electrochem. Soc. 168 (2021) 093501.
[33] S. Akiya, T. Kikuchi, S. Natsui, R.O. Suzuki, Optimum exploration for the self-ordering of anodic porous alumina formed via selenic acid anodizing, J. Electrochem. Soc. 162 (2015) E244.
[34] M. Iwai, T. Kikuchi, R.O. Suzuki, High-speed galvanostatic anodizing without oxide burning using a nanodimpled aluminum surface for nanoporous alumina fabrication, Appl. Surf. Sci. 537 (2021) 147852.
[35] F. Keller, M.S. Hunter, D.L. Robinson, Structural features of oxide coatings on aluminum, J. Electrochem. Soc. 100 (1953) 411.
[36] H. Shimada, M. Sakairi, H. Takahashi, Rise of breakdown potential of anodic oxide film on aluminum by pore filling method, J. Surf. Fin. Soc. Jpn. 53 (2002) 142.
[37] S.J. Garcia-Vergara, P. Skeldon, G.E. Thompson, H. Habazaki, A flow model of porous anodic film growth on aluminium, Electrochim. Acta 52 (2006) 681.
[38] J.E. Houser, K.R. Hebert, The role of viscous flow of oxide in the growth of self-ordered porous anodic alumina films, Nat. Mater. 8 (2009) 415.
[39] K.R. Hebert, S.P. Albu, I. Paramasivam, P. Schmuki, Morphological instability leading to formation of porous anodic oxide films, Nat. Mater. 11 (2012) 162.
[40] Ö.Ö. Çapraz, P. Shrotriya, P. Skeldon, G.E. Thompson, K.R. Hebert, Role of oxide stress in the initial growth of self-organized porous aluminum oxide, Electrochim. Acta 167 (2015) 404.
[41] P. Mishra, K.R. Hebert, Flow instability mechanism for formation of self-ordered porous anodic oxide films, Electrochim. Acta 222 (2016) 1186.
[42] P. Mishra, K.R. Hebert, Self-organization of anodic aluminum oxide layers by a flow mechanism, Electrochim. Acta 340 (2020) 135879.
[43] J. Oh, C.V. Thompson, The role of electric field in pore formation during aluminum anodization, Electrochim. Acta 56 (2011) 4044.
[44] T. Aerts, T. Dimogerontakis, I. De Graeve, J. Fransaer, H. Terryn, Influence of the anodizing temperature on the porosity and the mechanical properties of the porous anodic oxide film, Surf. Coat. Technol. 201 (2007) 7310.
[45] L. Zaraska, G.D. Sulka, M. Jaskuła, Anodic alumina membranes with defined pore diameters and thicknesses obtained by adjusting the anodizing duration and pore opening/widening time, J. Solid State Electrochem. 15 (2011) 2427.
[46] R. Kondo, T. Kikuchi, S. Natsui, R.O. Suzuki, Fabrication of self-ordered porous alumina via anodizing in sulfate solutions, Mater. Lett. 183 (2016) 285.
[47] G.E. Thompson, G.C. Wood, R. Hutchings, Porous anodic films formed on aluminium in chromic acid, Trans. IMF 58 (1980) 21.